Proceedings of the Fifth IIEEJ International Workshop
on Image Electronics and Visual Computing 2017
Da Nang, Vietnam, February 28- March 3, 2017

MULTIPLE SCATTERING SIMULATION OF LIGHT BEAM SHAFTS USING NARROW BEAM APPROXIMATION

Mikio Shinya[†] Takashi Yuasa Michio Shiraishi[‡]
[†]Toho University/UEI Research [‡]Toho University

ABSTRACT

This paper proposes an efficient and reasonably accurate method simulating multiply scattered light emitted from spot or beam light sources. This method utilizes the narrow beam theory, which analytically approximates multiple scattering phenomena for concentrated beam light sources. Although its naive straight-forward application does not allows satisfactory image synthesis, we successfully adopted the theory into a ray-marching scheme and obtained much improved results.

1. INTRODUCTION

Realistic rendering of participating media is necessary in many scenes. For example, shafts of light from headlights are important to render foggy night scenes. The light is scattered in participating media by particles, and we see bright particles that scatter light, forming shafts of light. The appearance of the shafts of light changes according to scattering properties such as density and albedo of the particles.

Although single scattering can be easily simulated by line integrals in real-time, rendering multiple scattering scenes has been hard to perform in real-time because this requires to solve the volumetric rendering equation. [1], Although the equation can be solved by stochastic methods such as Monte-Carlo ray-tracing and volume photon mapping [2], these methods are computationally expensive for real-time applications.

Recently, the narrow beam theory was introduced to the graphics field and successfully applied to image blurring due to multiple scattering [3]. Yuasa, et. al., attempted to apply the theory to shaft of light rendering [4]. Unfortunately, however, their direct application of calculated intensity distributions could not capture visual features of light shafts, as seen in later sections. This paper adopts a ray-marching scheme to improve the narrow beam solutions and applied to shaft of light rendering. We made comparisons between the results from the proposed method and path-tracing, and reasonable agreements were confirmed.

The main progress over the previous work is that we coupled the heuristic narrow beam function [3] with the ray-marching scheme and made significant improvements over the straightforward method [4].

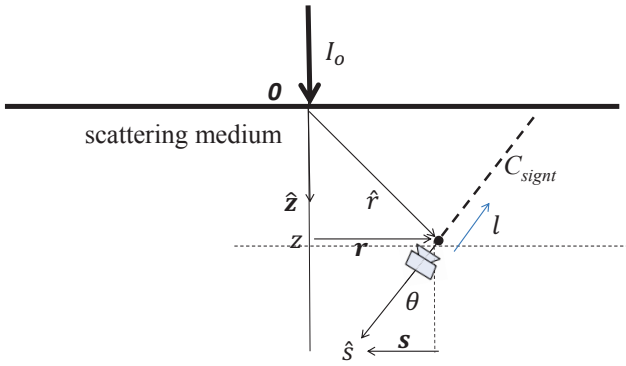

Figure 1: Coordinate system and experimental arrangement.

2. NARROW BEAM THEORY

This section gives a brief introduction to the narrow beam theory [5]. The major symbols used in the equations are listed in Table 1, and the associated coordinate system is shown in Figure 1.

The light transport equation for intensity $I(\hat{r}, \hat{s})$ can be expressed by

$$(\nabla \cdot \hat{s})I(\hat{r}, \hat{s}) = -(\rho_n \sigma_t)I(\hat{r}, \hat{s}) + (\rho_n \sigma_s) \int_{4\pi} p(\hat{s}, \hat{s}')I(\hat{r}, \hat{s}')d\hat{s}', \quad (1)$$

$$\int_{4\pi} p(\hat{s}, \hat{s}')d\hat{s}' = 1, \quad (2)$$

where $\hat{s}$ and $\hat{r}$ represent the direction and position in 3D, ρ_n is the density of the media, σ_t and σ_s are the extinction and scattering coefficients, and $p()$ is the phase function normalized to 1. The integral domain 4π indicates the unit sphere, and integral domains are infinite unless explicitly specified.

We set the intensity I to be the sum of the direct component I_{ri} and indirect component I_d

$$I = I_{ri} + I_d.$$

Let us assume that

Table 1: Symbols used in narrow beam theory.

$\hat{r}$, $\boldsymbol{r}$, z	position ($\hat{r} = \boldsymbol{r} + z\hat{z}$)
$\hat{s}$, $\boldsymbol{s}$	direction ($\hat{s} = \boldsymbol{s} + \hat{z}$)
σ_t	extinction coefficient
σ_s	scattering coefficient
σ_a	absorption coefficient ($\sigma_a = \sigma_t - \sigma_s$)
ρ_n	particle density
ζ	integral of ρ_n along path
τ	optical depth ($\tau = \sigma_t\zeta$)
$\boldsymbol{\kappa}$	Fourier variable corresponding to $\boldsymbol{s}$
$\boldsymbol{q}$	Fourier variable corresponding to $\boldsymbol{r}$
$p(\boldsymbol{s})$	phase function
$P(\boldsymbol{\kappa})$	Fourier transform of p
$I_0(\boldsymbol{r}, \boldsymbol{s})$	incident light distribution
$F_0(\boldsymbol{\kappa}, \boldsymbol{q})$	Fourier transform of I_0

- the intensity I is concentrated near the $\hat{z}$ direction (i.e., $\hat{s} \cdot \hat{z} = \cos\theta \simeq 1$);
- the variation in the phase function is smooth, allowing I_d to be approximated by a second-order Taylor expansion in direction $\hat{s}$ in the spherical integral in Equation (1).

Note that these assumptions may suffer accuracies in directional distributions as discussed in the next section.

We also assume the following situations to obtain explicit solutions:

- there is only one type of scattering particles in the media and σ_t, σ_s, and $p(\boldsymbol{s}, \boldsymbol{s}')$ do not change in space;
- the scattering media are structured into layers, and the particle density may change along the z axis, described as $\rho(z)$.

We set

$$\hat{r} = \boldsymbol{r} + z\hat{z}, \qquad \hat{s} \simeq \boldsymbol{s} + \hat{z},$$

where $\hat{z}$ is the unit vector in the z direction. Using this approximation, the spherical integral with $\hat{s}$ in Equation (1) can be approximated by a planar integral with a 2D vector $\boldsymbol{s}$. We also assume an axially symmetric phase function around the forward direction:

$$p(\boldsymbol{s}, \boldsymbol{s}') = p(|\boldsymbol{s} - \boldsymbol{s}'|). \tag{3}$$

Using these simplifications, the integro-differential equation in Equation (1) can be replaced by a second-order partial differential equation. Using Fourier transform, we can obtain the solution as

$$\begin{aligned} I_{ri}(z, \boldsymbol{r}, \boldsymbol{s}) &= 1/(2\pi)^4 \int_{-\infty}^{\infty} d\kappa \\ &\quad \int_{-\infty}^{\infty} \exp(-i\boldsymbol{\kappa} \cdot \boldsymbol{r}) \cdot \exp(-i\boldsymbol{s} \cdot \boldsymbol{q}) \cdot \\ &\quad F_0(\boldsymbol{\kappa}, \boldsymbol{q} + \boldsymbol{\kappa}z) \cdot \exp(-\sigma_t\zeta(z))dq, \qquad (4) \\ I_d(z, \boldsymbol{r}, \boldsymbol{s}) &= 1/(2\pi)^4 \exp(-\rho_n\sigma_a z) \int F_d(z, \boldsymbol{\kappa}, \boldsymbol{q} + \boldsymbol{\kappa}z) \cdot \\ &\quad \exp(-i\boldsymbol{s} \cdot \boldsymbol{q})dq \int \exp(-i\boldsymbol{\kappa} \cdot \boldsymbol{r})d\kappa, \qquad (5) \\ F_d(z, \boldsymbol{\kappa}, \boldsymbol{q}) &= \sigma_t F_0(\boldsymbol{\kappa}, \boldsymbol{q}) \int_0^z \rho_n(z')P(\boldsymbol{q} - z'\boldsymbol{\kappa}) \\ &\quad \exp(-\sigma_s\zeta(z')) \exp(-q^2\hat{A}(z, z'))dz', \qquad (6) \\ \zeta(z) &= \int_0^z \rho_n(z')dz', \qquad (7) \\ \tau(z) &= \sigma_t\zeta(z), \qquad (8) \\ \hat{A}(z, z') &= \int_{z'}^z A(z'')dz'', \qquad (9) \\ A(z) &= \rho_n(z)(\sigma_s/4) < \theta^2 >, \qquad (10) \\ < \theta^2 > &= \int_{4\pi} \theta^2 p(\boldsymbol{s})ds / \int_{4\pi} p(\boldsymbol{s})ds, \qquad (11) \end{aligned}$$

where $< \ . \ >$ represents an average, i indicates the imaginary unit, F_0 is the Fourier transform of the incident light distribution $I_0(\boldsymbol{r}, \boldsymbol{s})$

$$F_0(\boldsymbol{\kappa}, \boldsymbol{q}) = \int \exp(i\boldsymbol{q} \cdot \boldsymbol{s})ds \int I_0(\boldsymbol{r}, \boldsymbol{s}) \exp(i\boldsymbol{\kappa} \cdot \boldsymbol{r})dr,$$

and P is the Fourier transform of the phase function p. $\tau(z)$ indicates optical depth at z, and $\boldsymbol{\kappa}$ and $\boldsymbol{q}$ are the Fourier variables corresponding to $\boldsymbol{r}$ and $\boldsymbol{s}$, respectively. Integrals without a specified domain are planar integrals over the whole plane.

For more details, readers are invited to refer to the book of Ishimaru [5].

3. DISTRIBUTION FUNCTION FOR GAUSSIAN BEAMS

3.1. NARROW BEAM APPROXIMATION

In previous work [3], distribution functions for an incident ray were presented. Since we aim to evaluate the distribution of light emitted form a spot light source, let us assume a Gaussian light distribution as:

$$I_0(\boldsymbol{r}, s) = 1/(4\pi B_l) \exp(-|\boldsymbol{s}|^2/(4B_l))\delta(\boldsymbol{r}).$$

The phase function is assumed to be Gaussian and is set to

$$p(\boldsymbol{s}) = 1/(4\pi B) \exp(-|\boldsymbol{s}|^2/(4B)), \tag{12}$$

Then, both Fourier transforms have analytical forms, such that

$$\begin{aligned} F_0(\boldsymbol{\kappa}, q) &= \exp(B_l|\boldsymbol{\kappa}|^2), \qquad (13) \\ P(\boldsymbol{q} - z'\boldsymbol{\kappa}) &= \exp(-B(\boldsymbol{q} - z'\boldsymbol{\kappa})^2). \qquad (14) \end{aligned}$$

Putting these expressions into Equation (5) yields a line integral

$$\begin{aligned} I_d(z,r,s) &= K_G(z)\exp\left\{-|\boldsymbol{s}|^2/(4\Sigma_G^2)\right\}\cdot\pi^2 \\ &\int_0^z dz'\exp(-\rho_n\sigma_s z')/(\Sigma_G^2(z')\cdot C^2(z')) \\ &\exp\{-(\boldsymbol{r}+(-z+Bz'/\Sigma_G^2(z')\boldsymbol{s})^2 \\ &/(4C^2(z'))\}, \\ &= K_G(z)\cdot\pi^2 \\ &\int_0^z \exp(-s^2/(4\Sigma_G^2))\exp(-\rho_n\sigma_s z') \\ &1/(\Sigma_G^2(z')\cdot C(z')^2)\cdot \\ &\exp(-(\rho+(-z+(Bz'/\Sigma_G^2))s)^2/(4C^2))dz', \end{aligned} \tag{15}$$

where

$$\hat{A}(z,z') = (\sigma_t B)(\zeta(z)-\zeta(z')), \tag{16}$$
$$\Sigma_G^2(z') = B+B_l+\hat{A}(z,z'), \tag{17}$$
$$C^2(z') = Bz'^2[1-B/\Sigma_G^2], \tag{18}$$
$$K_G(z) = (1/2\pi)^4\sigma_s\exp(-\rho_n\sigma_a z). \tag{19}$$

The direct component I_{ri} can be calculated from

$$\begin{aligned} I_{ri}(z,\boldsymbol{r},\boldsymbol{s}) &= (1/4\pi B_l)(1/z^2)\delta(\rho/z-s) \\ &\exp(-s^2/(4B_l)\exp(-\tau(z)). \end{aligned} \tag{20}$$

Note that $\tau=(\rho_n\sigma_t)z$ when ρ_n is constant.

3.2. DIRECT INTEGRATION FOR BEAM SHAFTS

Eq. (15) suggests that, by setting $(\boldsymbol{r},z)$ as a camera position and $\hat{s}$ as the pixel direction, we can generate images of a light shaft by evaluating the integral. Yuasa, et. al., followed this idea and attempted image synthesis of spot light scenes. Fig. 4 shows synthesized images by (a) path-tracing (reference), (b) single scattering and (c) evaluations of Eq. (15). In (c), a circular bright spot is seen around the light source and very diffrent from that in the reference image (a). This is unnatural because the sight is almnost outside of the spot light.

This observation could be qualitatively understood in the following way. As descrived Section 2, the theory assumes that the changes in I_d be mild and can be quadratically approximated by:

$$\begin{aligned} I_d(z,\rho,s+s') &\simeq I_d(z,\rho,s)+s'\cdot\nabla_s I_d(z,\rho,s) \\ &+(1/2)(s'\cdot\nabla_s)^2 I_d(z,\rho,s). \end{aligned} \tag{21}$$

Since the direct integration Eq. (15) is a solution of partial differential equations based on the approximation Eq. (21), the calculated I_d is also a quadratic with respect to direction $\hat{s}$ in theory. Although, for example, the single scatteing component is very sharp and asymmeric with direction as shown in Fig. 4-(b), the direct integration cannot capture such features. This suggests that we cannot expect too much to Eq. (15) when variation in $\hat{s}$ is critical. Fortunately, previous work [3] found statistical values integrated over $\hat{s}$, such as averages and variances, can be well approximated by the theory through a heuristic function. Let us follow their approach.

3.3. HEURISTIC DISTRIBUTION FUNCTION

As described in [3], the zeroth- to second-order moments of I_d, M_i, can be easily estimated by line integrals, as:

$$M_0(z) = \exp(-\sigma_a\zeta(z))(1-\exp(-\sigma_s\zeta(z))), \tag{22}$$
$$M_1(z) = 0, \tag{23}$$
$$\begin{aligned} M_2(z) &= 4\int_0^z dz'(\rho_n(z')\sigma_s)\exp(-\sigma_s\zeta(z')) \\ &\left[C(z')^2+(z-Bz'/\Sigma_G^2(z'))^2\Sigma_G^2(z')\right]. \end{aligned} \tag{24}$$

It is also shown that the infinite integral of a Gaussian function (also known as the error function) G,

$$G(x) = 1/\sqrt{2\pi}\int_x^\infty \exp(u^2/2)du, \tag{25}$$

is a good approximation of the distribution function Ψ,

$$\Psi(z,\boldsymbol{r}) = \int I_d(\boldsymbol{r}-\boldsymbol{r}',\boldsymbol{s}')ds', \tag{26}$$

when it has the same moment values up to the second order [3]. This condition is satisfied by setting:

$$\Psi(z,\boldsymbol{r}) = \alpha(z)(1/|\boldsymbol{r}|)G(|\boldsymbol{r}|/\beta(z)) \tag{27}$$
$$\alpha(z) = 2M_0/\beta^2(z), \tag{28}$$
$$\beta^2(z) = 3(M_2(z)/M_0(z)). \tag{29}$$

Since $\Psi(z,\boldsymbol{r})$ is the total flux, we still need its angular distribution. It is known that the "multiply scattered phase function" approximates angular distribution after multiple scattering [6], defined as:

$$P_{MS}(\theta) = (1/N_{PM})p(\theta/\sqrt{1-\exp(-l)}), \tag{30}$$
$$d = z'+d_2, \tag{31}$$
$$l = \sigma_s d, \tag{32}$$
$$\hat{s} = (\hat{r}-\hat{r_z})/|\hat{r}-\hat{r_z}|, \tag{33}$$

and we set

$$I_d(z,\boldsymbol{r},\boldsymbol{s}) \simeq P_{MS}(\theta)\Psi(z,\boldsymbol{r}). \tag{34}$$

3.4. RAY MARCHING WITH THE HEURISTIC DISTRIBUTION FUNCTION

To improve the acuracy in directions, we couple the heuristic distribution function Eqs. (24) to (29) with the ray-marching equation. This, at least, enables to capture single scattering terms by integrating contributions from the direct light I_{ri}. In addition, we can generally expect further improvements in the following sense.

The light transport equation (1) can be solved iteratively, and the n-th solution is obtained by an integral over the sight line C_{sight} (Fig. 1), as:

$$\begin{aligned} I^{(n)} &= \int_{C_{sight}} [\exp(-d(l'))\sigma_s \int_{\Omega} p(s,s') \cdot \\ &\quad I^{(n-1)}(l',s')ds']dl' + I_0(l,s), \qquad (35) \\ &= \mathcal{L}I^{(n-1)}, \qquad (36) \end{aligned}$$

where $\mathcal{L}$ represents a linear integral operator that maps a function $I^{(n-1)}$ to $I^{(n)}$. The complete solution $I^{(\infty)}$ can be regarded as the fixed point of $\mathcal{L}$. By repeatedly applying $\mathcal{L}$ n-times to any function that satisfy the boundary condition, i.e., light sources, the approximated solution $I^{(n)}$ tends to the exact one $I^{(\infty)}$. This implies that, generally speaking, the operator $\mathcal{L}$ refines approximated solutions.

Applying the ray-marching operator $\mathcal{L}$ to the narrow beam solustion, $I_r + I_d$ yields:

$$\begin{aligned} I^{beam} &= \int_{C_{sight}} [\exp(-\tau(l'))\sigma_s(\int_{\Omega} p(s,s')I_{ri}ds') \\ &\quad + I_d]dl' + I_0(l,s). \qquad (37) \end{aligned}$$

This actually improves the acuracy and can be efficiently implemented as the next section describes.

4. METHOD

This section describes implimentation issues of the proposed method. To render shafts of light, we calculate the line integral, Eq. (37), per pixel. As shown in Fig. 2-(a), points $\hat{r}_i$ is sampled along the viewing ray path, and I_{ri} and I_d are calculeted to sum up the integral. We implemented this calculation in three steps:

- calculation of the beam parameters, $\alpha(z)$ and $\beta(z)$, accroding to Eqs. (28) and (29),
- setting the integration interval $\hat{r}_0$ to $\hat{r}_n$,
- calculate $I_{ri}(\hat{r}_i)$ and $I_d(\hat{r}_i)$ according to Eq. (34) and sum them up.

The first step was implemented on a CPU as a pre-process, while the second and third ones on a GPU executed every frame. To reduce unnecessary integral computation, we set a boundary tube and evaluate the integral only inside the tube.

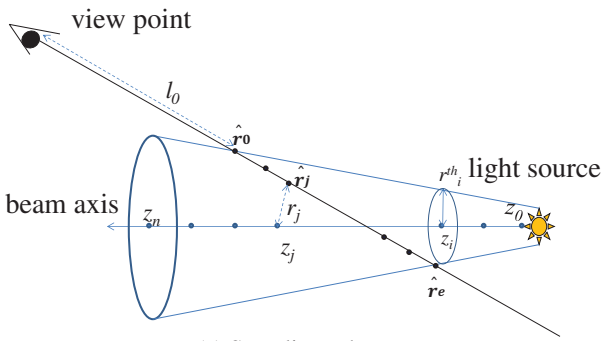

(a) Sampling scheme.

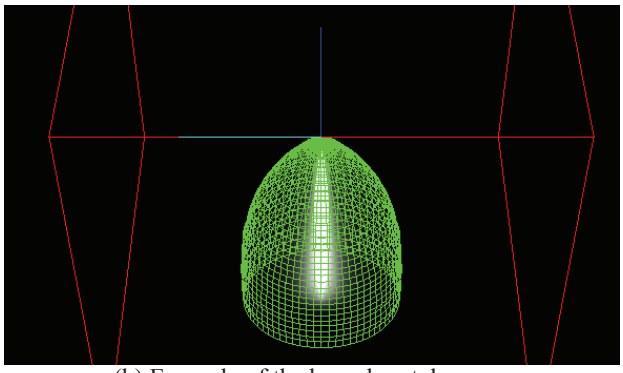

(b) Example of the boundary tube.

Figure 2: Sampling scheme and the boundary tube example.

4.1. PRE-PROCESS

For each light beam, we descretize the beam axis, and at sample point z_i, we evaluate beam parameters using Eqs. (24), (28) and (29). Although it is desireable to incrementally sum up the moment at z_i, $M_2(z_i)$ as:

$$M_2(z_{i+1}) = M_2(z_i) + \delta M_2, \qquad (38)$$

the incremental term δM_2 depends on all $0 < z < z_i$ as:

$$\begin{aligned} \delta M_2 &= \sum_{j=0}^{i} (\rho_n(z_j)\sigma_s) \exp(-\sigma_s \zeta(z_j))[C(z_i)^2 \\ &\quad + (z_i - Bz_j/\Sigma_G^2(z_j))^2 \Sigma_G^2(z_j))]\delta_z, \qquad (39) \end{aligned}$$

where δ_z is the sampling interval. This apparently involves i-times calculations for the i'th evaluation, and thus, naive implimentations cost $O(n^2)$ to evaluate it from z_0 to z_n. Fortunately, however, we can re-organize Eq. (39), so as to allow us to evaluate in a linear order.

Putting Eqs. (18) and (17) into Eq. (39) and arranging terms according to dependencies on z_j yields:

$$\begin{aligned}
\delta M_2(z_i) &= (B + B_l + \sigma_s B\zeta(z_i))F_1 + \\
&\quad (-2Bz)F_2 + BF_3 + (-\sigma_s Bz^2)F_4 && (40)\\
F_1(z_i) &= \sum_{j=0}^{i} E_0\delta_z, && (41)\\
F_2(z_i) &= \sum_{j=0}^{i} E_0 z_j\delta_z, && (42)\\
F_3(z_i) &= \sum_{j=0}^{i} E_0 z_j^2\delta_z, && (43)\\
F_4(z_i) &= \sum_{j=0}^{i} E_0\zeta(z_j)\delta_z, && (44)\\
E_0 &= \rho(z_j)\sigma_s \exp(-\sigma_s * \zeta(z_j)). && (45)
\end{aligned}$$

Using these formulae, the integral can be performed in an incremental manner by:

$$\begin{aligned}
F_1(z_i) &= E_0\delta_z + F_1(z_{i-1}), && (46)\\
F_2(z_i) &= E_0 z_i\delta_z + F_2(z_{i-1}), && (47)\\
F_3(z_i) &= E_0 z_i^2\delta_z + F_3(z_{i-1}), && (48)\\
F_4(z_i) &= \zeta(z_i)\delta_z + F_4(z_{i-1}), && (49)\\
\delta M_2(z_i) &= ((B + B_l) + \sigma_s B\zeta(z_i))F_1(z_i) + \\
&\quad (-2Bz)F_2(z_i) + BF_3(z_i) + \\
&\quad (-\sigma_s Bz^2)F_4(z_i) && (50)\\
M_2(z_i) &= M_2(z_{i-1}) + \delta M_2, && (51)\\
M_0(z_i) &= \exp(-\sigma_a\zeta(z_i)) \\
&\quad (1 - \exp(-\sigma_s\zeta(z_i))) && (52)
\end{aligned}$$

The beam parameters at z_i are then calculated by:

$$\begin{aligned}
\beta^2(z_i) &= 3(M_2(z_i)/M_0(z_i)) && (53)\\
\alpha(z_i) &= 2M_0(z_i)/\beta^2(z_i). && (54)
\end{aligned}$$

This step also determines the boundary tube that specifies the integral intervals. Given a threshold Ψ_{th}, we search the smallest radius r_i^{th} such that:

$$\Psi(z_i, r_i^{th}) < \Psi_{th}, \quad (55)$$

for each z_i and construct the boundary tube using r_i^{th} as the radius of the tube at z_i. Fig. 2-(b) shows an example.

4.2. RUN-TIME PROCESS

The run-time process was implemented on a GPU in two passes. In the first pass, we draw the boundary tubes from the view point and keep their maximum and minimum depths. In the second pass, we set up the integral interval l_0 and l_e at each pixel according to the maximum/minimum boundary depth values. Then, the integral is evaluated by summing up

$$\begin{aligned}
I^{beam} &= \sum_i [\exp(-\tau(l_i))\sigma_s(p(s, s_0)I_{ri}(l_i) + \\
&\quad I_d(z_i, \boldsymbol{r}_i)]\delta_l && (56)\\
I_d(z_i, \hat{r}_i) &\simeq P_{MS}\Psi(z_i, \boldsymbol{r}_i) && (57)\\
\Psi(z_i, \hat{r}_i) &= \alpha(z_i)(1/|\boldsymbol{r}_i|)G(|\boldsymbol{r}_i|/\beta(z_i)), && (58)\\
\hat{r}_i &= l_i\hat{s} + \hat{e} && (59)
\end{aligned}$$

where $\hat{e}$ and l_i denotes the view point and the distance between the view point and sample point, and δ_l represents the sampling interval.

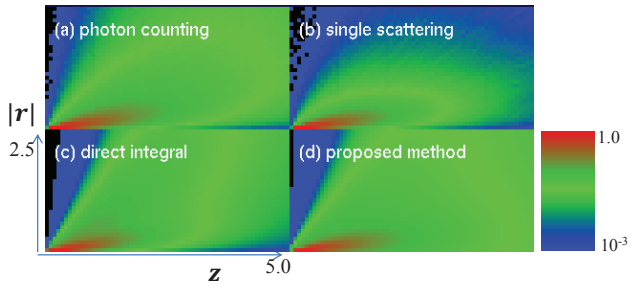

Figure 3: Comparisons of calculated distribution functions (Ψ). $\sigma_t = 1.0$, $\sigma_s = 0.95$, and $d\theta = 40$ degs.

5. EXPERIMENT

We evaluated distribution functions Ψ by: (a) photon counting (reference), (b) single scattering, (c) direct integration of Eq. (15), (d) the proposed method based on Eq. (27). Fig.3 shows as color-coded the distributions measured by the four methods. As seen in the figure, the proposed method provides a much better result (RMS= 0.20) than those from the direct integral (RMS= 0.31) and from the single scattering method (RMS= 0.36).

Fig.4 shows rendered images of a beam in a uniform scattering medium by: (a) path-tracing, (b) the direct calculation (Eq. (15)), (c) the single-scattering approximation, and (d) the proposed method. As seen in the figure, although the direct calculation does not provide good approximation, the proposed method created better result (RMS=0.18).

We implemented the method on a GPU. Fig.5 shows an example result, showing a city with red laser beams shooting upperward. The computation time was 160 msec for light shaft rendering (90 msec for other rendering), on a Windows PC (Intel Core i7-3770K @3.50GHz, GeForce GTX 690), at the resolution of 640 $\times$ 480. We consider

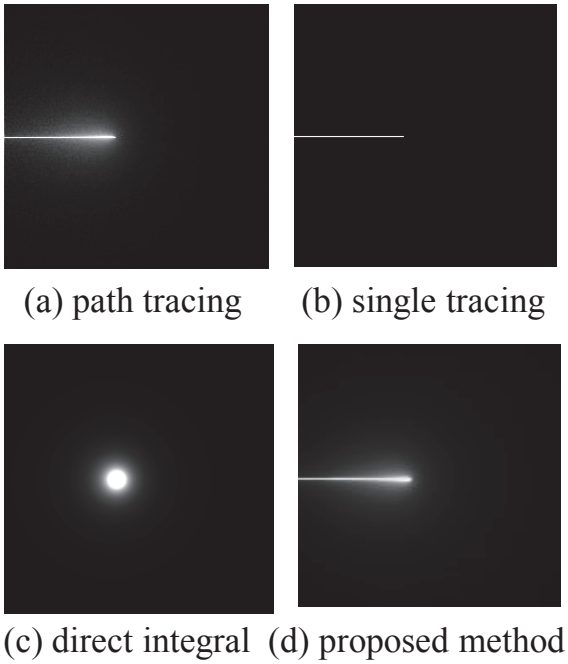

Figure 4: Comparisons of generated images of a shaft of light. A beam source is located in left-middle of the image. $\sigma_t = 1.0$, $\sigma_s = 0.95$, and $d\theta = 40$ degs.

it possible to reduce the computation cost by tightening the boundary tube, which is currently rather loose (Fig. 2-(b)). We also consider that another important factor would be sampling strategies of the integral. Although we currently apply a simple uniform sampling, better adaptive sampling could reduce the number of samples while avoiding aliasing artifacts.

There are a few limitations on the method. The method only deal with a Gaussian or sum of Gaussian beams and can not handle sharp-cut spot lights. Another limitation is that the method does not correctly handle shadowing: it simply skip shadowing regions from the integral intervals. Future stadies include to ease these limitations in addition to further acceleration of the method.

6. CONCLUSION

This paper proposed an efficient and reasonably accurate method simulating multiply scattered light emitted from spot and beam light sources. This method utilizes the narrow beam theory, which analytically approximates multiple scattering phenomena for concentrated beam light sources. Although naive applications of the theory does not allows satisfactory image synthesis, we successfully adopted the theory into a ray-marching scheme and obtained much improved results.

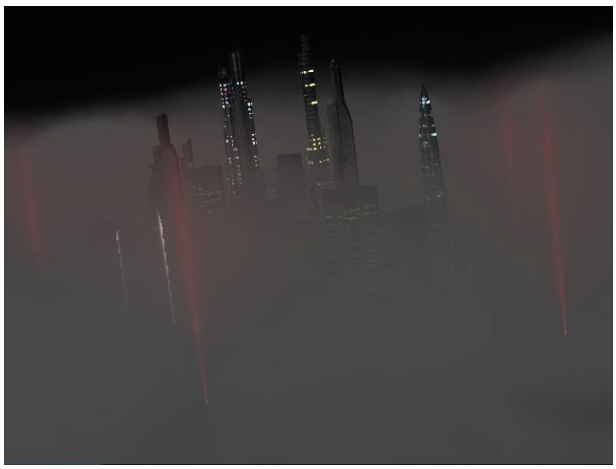

Figure 5: An example image generated by the proposed method.

[1] J. T. Kajiya, The rendering equation, SIGGRAPH'86, No. 4, pp. 143-150, 1986.

[2] H. W. Jensen, Realistic image synthesis using photon mapping, A. K. Peters, 2001.

[3] M. Shinya, Y. Dobashi, M. Shiraishi, M. Kawashima, T. Nishita, Multiple Scattering Approximation in Heterogeneous Media by Narrow Beam Distributions, Computer Graphics Forum, Vol. 35, No. 7, pp 373-382.

[4] T. Yuasa, M. Shinya, M. Shiraishi, Visual simulation of multiple scattering in spot light illumination, IWAIT2016, 1B-3, 2016.

[5] A. Ishimaru, Wave propergation and scattering in random media, volume 1, Academic Press, New York, 1978.

[6] S. Premoze, M. Ashikhmin, P. Shirley, Path Integration for Light Transport in Volumes, Eurographics Symposium on Rendering, pp. 1-12, 2003.